Tripod Self-Assembled Monolayer on Au(111) Prepared by Reaction of Hydroxyl-Terminated Alkylthiols with SiCl 4

ARTICLE *in* LANGMUIR · APRIL 2008

Impact Factor: 4.46 · DOI: 10.1021/la703196b · Source: PubMed

3 AUTHORS, INCLUDING:

Andrew S Ichimura
San Francisco State University
44 PUBLICATIONS **862** CITATIONS

SEE PROFILE

David L Allara
Pennsylvania State University
261 PUBLICATIONS **23,293** CITATIONS

SEE PROFILE

Tripod Self-Assembled Monolayer on Au(111) Prepared by Reaction of Hydroxyl-Terminated Alkylthiols with $SiCl_4$

Andrew S. Ichimura,*,† Wanda Lew,† and David L. Allara*,‡

Department of Chemistry and Biochemistry, San Francisco State University, 1600 Holloway Avenue, San Francisco, California 94132, and Department of Chemistry, Pennsylvania State University, University Park, Pennsylvania 16802

Received October 15, 2007. In Final Form: December 1, 2007

Infrared reflection spectroscopy (IRS), single wavelength ellipsometry, and density functional theory were used to elucidate the structure of a molecular tripod self-assembled monolayer (SAM) on polycrystalline gold{111} substrates. The tripod SAM was formed by the reaction of $SiCl_4$ with a densely packed monolayer of 2-mercaptoethanol, 6-mercaptohexanol, and 16-mercaptohexadecanol under inert atmosphere. After reaction with $SiCl_4$, IRS spectra show an intense absorption at ∼1112 cm^{-1} that is attributed to Si−O−C asymmetric stretching vibration of a molecular tripod structure. Harmonic vibrational frequencies computed at the B3LYP/6-311+g** level of theory for the mercaptoethanol tripod SAM closely match the experimental IRS spectra, giving further support for the tripod structure. When rinsed with methanol or water, the Si−Cl-terminated SAM becomes capped with Si−OMe or Si−OH. The silanol-terminated tripod SAM is expected to find use in the preparation of thin zeolite and silica films on gold substrates.

Introduction

The ability to design and synthesize custom surfaces with specific properties through chemical processes, such as the adsorption of organic thiols on gold and subsequent transformations of the tail groups, is one of the primary motivations for developing novel self-assembled monolayers (SAM).[1] Functionalized SAMs have promise for applications in areas as diverse as materials science and chemical biology and are important systems for fundamental studies at the nanoscale.[1,2] One area of research where the development of new monolayers has received little attention is their use for the growth of zeolite films.

Supported zeolite films have received considerable attention recently because of their potential applications as sensors,[3−8] low-*k* dielectrics,[9−11] and size-selective electrodes.[12,13] Our interest in zeolite films stems from the intriguing optical and electrical properties that result when alkali metals (M═Na−Cs) are added to pure silica zeolites (SZ), such as ITQ-4 or zeolite beta.[14−16] The significant feature of alkali metal doped silica zeolites, M@SZ, is that the alkali metal ionizes within the zeolite channels to yield electrons confined to the zeolite pores and a stoichiometric number of cations. Because the 'excess' electrons are located within the zeolite channels, a metal-doped zeolite with a one-dimensional channel structure, such Cs@ITQ-4,[14−16] may be a low-dimensional metal, as predicted by density functional theory (DFT).[17] Previous experimental work has focused on the properties of bulk powders. However, the preparation of supported M@SZ thin films would facilitate an experimental study of the charge transport properties and cast them in a form suitable for later applications. For our work, gold on silicon supports are of particular interest because of their well-known and reproducible surface characteristics. In addition, the gold layer may be advantageous for future conductivity measurements through the zeolite film.

A well-developed route to grow zeolite films (especially MFI) on gold begins with the formation of a 3-mercaptopropyltrimethoxysilane SAM.[18−25] In this method, the monolayer is first cross-linked by acid hydrolysis and then a cationic polymer is deposited on the resulting siloxane film to reverse the surface charge, which facilitates the adsorption of zeolite seed crystals. Secondary growth under hydrothermal synthesis conditions then

* To whom correspondence should be addressed. E-mail: ichimura@sfsu.edu (D.L.A.); dla@psu.edu (A.S.I.).

† San Francisco State University.

‡ Pennsylvania State University.

(1) Love, J. C.; Estroff, L. A.; Kriebel, J. K.; Nuzzo, R. G.; Whitesides, G. M. *Chem. Rev.* **2005**, *105*, 1103−1169.

(2) Swalen, J. D.; Allara, D. L.; Andrade, J. D.; Chandross, E. A.; Garoff, S.; Israelachvili, J.; McCarthy, T. J.; Murray, R.; Pease, R. F.; Rabolt, J. F.; Wynne, K. J; Yu, H. *Langmuir* **1987**, *3*, 932−950.

(3) Bein, T. *Chem. Mater.* **1996**, *8*, 1636−1653.

(4) Wang, Z. Z.; Larsson, M. L.; Grahn, M.; Holmgren, A.; Hedlund, J. *Chem. Comm.* **2004**, 2888−2889.

(5) Yan, Y.; Bein, T. *Chem. Mater.* **1992**, *4*, 975−977.

(6) Yan, Y.; Bein, T. *J. Phys. Chem.* **1992**, *98*, 9387−9393.

(7) Bein, T. *Chem. Mater.* **1999**, *8*, 1636−1653.

(8) Zhang, J.; Luo, M.; Xiao, H.; Dong, J. *Chem. Mater.* **2006**, *18*, 4−6.

(9) Li, Z.; Lew, C. M.; Li, S.; Medina, D. I.; Yan, Y. *J. Phys. Chem. B* **2005**, *109*, 8652−8658.

(10) Wang, Z.; Mitra, A.; Wang, H.; Huang, L.; Yan, Y. *Adv. Mater.* **2001**, *13* (19), 1463−1466.

(11) Li, S.; Li, A.; Medina, D.; Lew, C.; Yan, Y. *Chem. Mater.* **2005**, *17*, 1851−1854.

(12) Kornic, S.; Baker, M. *Chem. Comm.* **2002**, 1700−1701.

(13) Zhang, Y.; Chen, F.; Shan, W.; Zhuang, J.; Dong, A.; Cai, W.; Tang, Y. *Micropor. Mesopor. Mater.* **2003**, *65*, 277−285.

(14) Ichimura, A. S.; Dye, J. L.; Camblor, M. A.; Villaescusa, L. A. *J. Am. Chem. Soc.* **2002**, *124*, 1170−1171.

(15) Wernette, D. P.; Ichimura, A. S.; Urbin, S. A.; Dye, J. L. *Chem. Mater.* **2003**, *15* (7), 1441−1448.

(16) Petkov, V.; Billinge, S. J. I.; Vogt, T.; Ichimura, A. S.; Dye, J. L. *Phys. Rev. Lett.* **2002**, *89* (7), 75502−75506.

(17) Li, Z.; Yang, J.; Hou, J. G.; Zhu, Q.; *J. Am. Chem. Soc.* **2003**, *125*, 1170−1171.

(18) Tavolaro, A.; Drioli, E. *Adv. Mater.* **1999**, *11* (12), 975−996.

(19) Bein, T.; Brown, K.; Frye, G. C.; Brinker, C. J. *J. Am. Chem. Soc.* **1989**, *111*, 7640−7641.

(20) Yan, Y.; Bein, T. *J. Am. Chem. Soc.* **1995**, *117*, 9990−9994.

(21) Mihailova, B.; Engstrom, V.; Hedlund, J.; Holmgren, A.; Sterte, J. *Microporous Mater.* **1999**, *32*, 297−304.

(22) Mihailova, B.; Engstrom, V.; Hedlund, J.; Holmgren, A.; Sterte, J. *J. Mater. Chem.* **1997**, *9*, 1507−1510.

(23) Mintova, S.; Valtchev, V.; Engstrom, V.; Schoeman, B. J.; Sterte, J. *Microporous Mater.* **1997**, *11*, 149−160.

(24) Mintova, S.; Schoeman, B. J.; Valtchev, V.; Sterte, J.; Mo, S.; Bein, T. *Adv. Mater.* **1997**, *9* (7), 585−589.

(25) Engstrom, V.; Mihailova, B.; Hedlund, J.; Holmgren, A.; Sterte, J. *Microporous Mater.* **2000**, *38*, 51−60.

10.1021/la703196b CCC: $40.75
Published on Web 02/07/2008

Scheme 1

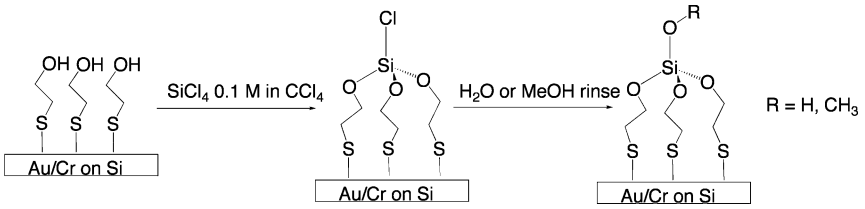

yields a continuous polycrystalline zeolite film. A disadvantage of using 3-mercaptopropyltrimethoxysilane as the interfacial layer is that this molecule does not form densely packed monolayers because of steric interactions between adjacent trimethoxysilane tail groups.[22] Defects due to less than optimal packing within the SAM are undesirable for future conductivity studies of alkali metal-doped zeolite films. Therefore, despite the success of this approach, a more general route was sought to chemically bind the zeolite film to the gold surface. It is envisioned that an improved method would (1) be based on densely packed and highly organized SAMs, (2) allow the interfacial layer to moderate the capacitance between the gold and zeolite by varying the length and nature of the organic monolayer, and (3) serve as the nucleation point for the growth and chemical attachment of zeolite films without the need for seeding.

A suitable monolayer would be composed of a thiol head group, an alkyl, aryl, or other composite molecular spacer, and a terminal Si−O−R functional group, where R may be hydrogen, methyl, or other labile functional group. To realize such a monolayer, we considered the sequence of reactions illustrated in Scheme 1. A SAM is initially prepared from α-hydroxy-terminated alkyl or aryl thiol molecules. Mercaptoethanol is used as an example. Exposure of the α-hydroxy-terminated SAM to silicon tetrachloride results in the formation of three Si−O−C bonds accompanied by loss of 3 equiv of HCl(g). Because of the reactive nature of $SiCl_4$ with hydroxyl groups, the result is predicted to be a molecular tripod anchored to the gold surface by means of three thiolate bonds. In the absence of water or other nucleophiles, the tripod SAM would be terminated with a Si−Cl bond that is oriented normal to the substrate surface. A water or methanol rinse results in a silanol- or methoxy-terminated tripod SAM, which should form a suitable substrate for zeolite film growth.

In this report, we present evidence for the molecular tripod structure formed by the reaction of mercaptoethanol (ME), 6-mercaptohexanol (MH), and 16-mercaptohexadecanol (MHD) with silicon tetrachloride. At each step in Scheme 1, the SAMs were studied by infrared reflection spectroscopy (IRS) and single wavelength ellipsometry (SWE) to determine the film thickness. DFT calculations were undertaken to provide a physical picture of the molecular tripod and to compare computed vibrational frequencies and the molecular thickness with experiment.

Experimental Methods

Single-side polished Si(100) wafers were soaked in H_2SO_4 (concd)/H_2O_2 (30%) [v/v = 4:1] solution at 85 C for 15 min, thoroughly rinsed with deionized water and ethanol, and dried under a stream of nitrogen. The clean silicon wafers were transferred to a bell jar, evacuated to 1×10^{-8} Torr, and then chromium (5−10 nm) and gold (200 nm) layers were deposited sequentially onto the polished wafers by thermal evaporation of the base metals. SAMs were prepared by placing the freshly deposited gold substrates into 2 mM solutions of the α-hydroxy-terminated alkyl thiols in anhydrous ethanol for 1−4 days. The reaction with silicon tetrachloride was carried out in a closed Teflon container within a nitrogen-purged glove bag by immersing the α-hydroxy-terminated SAMs in a 0.1−0.2 M solution of $SiCl_4$ in dry CCl_4 for 10 min. The wafers were then removed from the solution, rinsed with four 10 mL aliquots of dry CCl_4, and dried under nitrogen. The SAMs were characterized by IRS at a grazing angle of 86° with p-polarized light (800 scans, 2 cm^{-1} resolution), which employed a deuterated octadecanethiol ($HSC_{18}D_{37}$) SAM on gold as a reference, and SWE at a wavelength of 632.8 nm and fixed angle of 70° (Gaertner Scientific, model LSE). Calculations of the monolayer thickness assumed a value of 1.5 for the index of refraction and zero for the absorption coefficient.

DFT calculations of mercaptoethanol and the Si−Cl-terminated molecular tripod employed the B3LYP functional,[26−29] the 6-311+g** basis for H, C, O, Si, S, and Cl atoms,[30,31] and the LANL2DZ effective core potential (ECP) basis for gold.[32−34] In order to constrain the motion of the tripod during optimization, the tripod was anchored to a model gold (111) surface consisting of a single layer of 12 gold atoms ($[Xe]6s^{1}5d^{10}4f^{14}$) placed at the equilibrium distances of the bulk solid. Sulfur atoms, with thiol hydrogen atoms removed, were placed in the center of 3-fold hollows in a manner consistent with the commonly accepted structure of alkyl thiols on gold.[1] The positions of the gold atoms were fixed, and only the sulfur−gold surface distance was allowed to vary. All other bonding parameters were fully optimized under the constraint of C_3 symmetry. Because of the structural constraints imposed on the model surface, the computed stationary points on the potential energy surface were not expected to be true energy minima. The Si−Cl terminated tripod structure was optimized in both the doublet open-shell state using the unrestricted DFT formalism and the closed-shell singlet state using the restricted B3LYP functional by adding an electron to the molecule so that the highest-occupied molecular orbital contained two electrons. The open-shell state results from the removal of the thiol H atoms, which leaves three thiyl radicals bound to the model gold surface. The structure and frequencies of 2-mercaptoethanol in the gas phase were also computed with the B3LYP/6-311+g** model chemistry. The Gaussian03[35] suite of programs was used to optimize the geometries and compute harmonic vibrational frequencies.

(26) Becke, A. D.; *J. Chem. Phys.* **1993**, *98*, 5648.
(27) Vosko, S. H.; Wilk, L.; Nusair, M. *Can. J. Phys.* **1980**, *58*, 1200.
(28) Lee, C.; Yang, W.; Parr, R. G. *Phys. Rev. B* **1988**, *37*, 785.
(29) Miehlich, B.; Savin, A.; Stoll, H.; Preuss, H. *Chem. Phys. Lett.* **1989**, *157*, 200.
(30) McLean, A. D.; Chandler, G. S.; *J. Chem. Phys.* **1980**, *72*, 5639.
(31) Krishnan, R.; Binkley, J. S.; Seeger, R.; Pople, J. A. *J. Chem. Phys.* **1980**, *72*, 650.
(32) Hay, P. J.; Wadt, W. R. *J. Chem. Phys.* **1985**, *82*, 270.
(33) Wadt, W. R.; Hay, P. J. *J. Chem. Phys.* **1985**, *82*, 284.
(34) Hay, P. J.; Wadt, W. R. *J. Chem. Phys.* **1985**, *82*, 299.
(35) Frisch, M. J.; Trucks, G. W.; Schlegel, H. B.; Scuseria, G. E.; Robb, M. A.; Cheeseman, J. R.; Montgomery, J. A., Jr.; Vreven, T.; Kudin, K. N.; Burant, J. C.; Millam, J. M.; Iyengar, S. S.; Tomasi, J.; Barone, V.; Mennucci, B.; Cossi, M.; Scalmani, G.; Rega, N.; Petersson, G. A.; Nakatsuji, H.; Hada, M.; Ehara, M.; Toyota, K.; Fukuda, R.; Hasegawa, J.; Ishida, M.; Nakajima, T.; Honda, Y.; Kitao, O.; Nakai, H.; Klene, M.; Li, X.; Knox, J. E.; Hratchian, H. P.; Cross, J. B.; Bakken, V.; Adamo, C.; Jaramillo, J.; Gomperts, R.; Stratmann, R. E.; Yazyev, O.; Austin, A. J.; Cammi, R.; Pomelli, C.; Ochterski, J. W.; Ayala, P. Y.; Morokuma, K.; Voth, G. A.; Salvador, P.; Dannenberg, J. J.; Zakrzewski, V. G.; Dapprich, S.; Daniels, A. D.; Strain, M. C.; Farkas, O.; Malick, D. K.; Rabuck, A. D.; Raghavachari, K.; Foresman, J. B.; Ortiz, J. V.; Cui, Q.; Baboul, A. G.; Clifford, S.; Cioslowski, J.; Stefanov, B. B.; Liu, G.; Liashenko, A.; Piskorz, P.; Komaromi, I.; Martin, R. L.; Fox, D. J.; Keith, T.; Al-Laham, M. A.; Peng, C. Y.; Nanayakkara, A.; Challacombe, M.; Gill, P. M. W.; Johnson, B.; Chen, W.; Wong, M. W.; Gonzalez, C.; Pople, J. A. *Gaussian 03*, revision C.02; Gaussian, Inc.: Wallingford, CT, 2004.

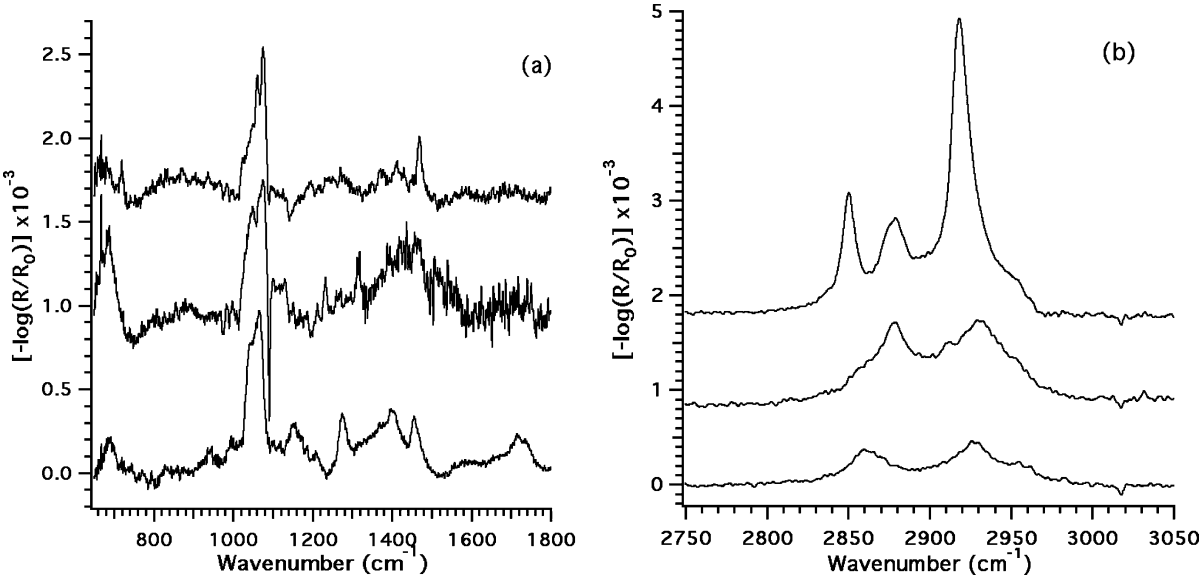

Figure 1. IRS spectra of mercaptoethanol (bottom), 6-mercaptohexanol (middle), and 16-mercaptohexadecanol (top) SAMs in the (a) low and (b) CH_2 stretching frequency regions. The spectra are shifted vertically for clarity.

Results and Discussion

The IRS spectra of mercaptoethanol, 6-mercaptohexanol, and 16-mercaptohexadecanol SAMs are shown in Figure 1. A comparison of the band positions, lineshapes, and intensities reveals that these monolayers are structurally similar. The C−O stretching band observed at 1067 (ME) and 1075 cm^{-1} (MH and MHD) is the most intense feature in the low-frequency region, Figure 1a. The CH_2 wagging, twisting, and scissoring deformation bands occur between 1180 and 1470 cm^{-1}.[36] These bands are well resolved in the ME SAM but are broader and more intense than the corresponding features in the MH and MHD spectra. The peak maxima also differ slightly. For example, the IRS spectrum of MHD exhibits a sharp resonance at 1470 cm^{-1} due to the CH_2 scissoring deformation,[36] whereas this band occurs at 1457 cm^{-1} in ME and ∼1465 cm^{-1} for MH. The methylene symmetric and asymmetric stretching bands of the ME SAM appear at 2860 and 2928 cm^{-1}, respectively, Figure 1b. The corresponding bands of MHD are observed at 2851 and 2919 cm^{-1}. The spectrum of MHD has an additional feature at 2878 cm^{-1} that is due to partial disorder at the α-CH_2 next to the hydroxyl tail group.[37] The CH_2 asymmetric stretching band of 6-mercaptohexanol is observed 2930 cm^{-1}, while the symmetric band appears as a shoulder at ∼2860 cm^{-1}. The feature at 2878 cm^{-1} in the MH monolayer is also due to disorder at the tail group. The similarity of the ME and MH IRS spectra to that of MHD suggests that the ME and MH SAMs are densely packed and adopt dominant trans conformations. It should be noted that mercaptoethanol required a 4 day maturation period in ethanol solution for triplicate samples to yield identical IRS spectra and film thicknesses. As expected, the observed CH_2 stretching vibrations of ME and MH SAMs confirm that these SAMs have a less organized nature rather than the quasi-crystalline two-dimensional order that is typical of SAMs formed with long-chain alkane thiols, such as, 16-mercaptohexadecanol.[38,39] The spectral shifts and broader lineshapes in the 1180−1470 cm^{-1} region of the ME and MH monolayers also suggest a greater degree of disorder relative to the MHD SAM. The observed vibrational frequencies and their assignments are collected in Table 1.

The IRS spectra of the ME, MH, and MHD SAMs after reaction with silicon tetrachloride, Figure 2 and Table 1, show that significant structural changes occurred especially at the hydroxyl tail group. In Figure 2a, the intense feature at 1117, 1112, and 1112 cm^{-1} is assigned to the Si−O−C asymmetric stretching vibration of the ME, MH, and MHD monolayers, respectively.[40,41] Notable changes also occur in the CH_2 vibrational modes. In the low-frequency region, the CH_2 twisting, rocking, and scissoring bands become broader and more intense after reaction with $SiCl_4$ indicating a change in molecular conformation. The band at 2878 cm^{-1} due to the disordered $-CH_2OH$ group in the MH and MHD spectra decreases and reveals the underlying symmetric CH_2 stretch at 2860 cm^{-1} of the MH spectrum. In the IRS spectrum of MHD, the CH_2 asymmetric vibration shifts to 2924 cm^{-1} and its full width at half-maximum line width increases to 32 from 16 cm^{-1} before reaction with $SiCl_4$. The CH_2 symmetric stretch experiences a slight frequency shift to 2852 cm^{-1} and the line width increases to 19 cm^{-1} compared to 12 cm^{-1} before reaction.

After reaction of the Si−Cl tripod with anhydrous methanol, Figure 3 and Table 1, the Si−O−C asymmetric stretch shifts slightly to 1105, 1110, and 1108 cm^{-1} for the ME, MH, and MHD monolayers, respectively. The reaction with methanol produces a distinct band at 2980 cm^{-1} in the ME tripod SAM spectrum, Figure 3b, and shoulders at the same frequency in the spectra of MH and MHD tripod SAMs. This frequency is consistent with a CH_3 asymmetric stretching vibration of a silyl methyl ether functional group.[40] In addition, new bands at 800 and 847 cm^{-1} appear in the spectra of the MH tripod SAM. These bands may be assigned to the symmetric and asymmetric rocking modes of the CH_3 group of Si−O−CH_3.[40] In the spectrum of the ME tripod SAM, the CH_3 rocking modes at ∼800 and ∼840 cm^{-1} are partially obscured by the background, while the corresponding bands for the MHD tripod occur at 794 and 844 cm^{-1} accompanied by an unidentified peak at 821 cm^{-1}. The

(36) Nuzzo, R. G.; Dubois, L. H.; Allara, D. L. *J. Am. Chem. Soc.* **1990**, *112*, 558−569.

(37) Moses Pei-Tien, H. Characterization of the structure and bonding of adsorbates on model silica surfaces. Ph.D. dissertation, The Pennsylvania State University, 1993.

(38) Porter, M. D.; Bright, T. B.; Allara, D. L.; Chidsey, C. E. D. *J. Am. Chem. Soc.* **1987**, *109*, 3559−3568.

(39) Alves, C. A.; Smith, E. L.; Porter, M. D. *J. Am. Chem. Soc.* **1992**, *114*, 1222−1227.

(40) Socrates, G. *Infrared Characteristic Group Frequencies*; John Wiley and Sons, Ltd.: New York, 1980.

Table 1. Observed Vibrational Frequencies of the 2-mercaptoethanol (ME), 6-mercaptohexanol (MH), 16-mercaptohexadecanol (MHD) SAMs and Their Products of Reaction with $SiCl_4$, and after Washing with MeOH. Also Tabulated Are the DFT Frequencies of ME and the ME Tripod SAMs.

	frequency (cm^{-1})				
sample	ME	MH	MHD	DFT[a,b]	assignment
				750	S−C str.
−OH	1067	1076	1076	1053	C−O str.
terminated	1276−1401	1200−1436	1180−1400[c]	1210−1444	CH_2 wag, twist
SAM	1457	1464	1472	1493, 1527	CH_2 scissors def
	2860	2860	2851	2992	CH_2 sym. str.
	2928	2931	2919	3026	CH_2 asym. str.
				505 (503)[d]	Si−Cl str
Si−Cl	1117	1112	1112	1106	Si−O−C asym. str.
terminated	∼1200−1400	∼1200−1400	∼1200−1400	1202−1398	CH_2 twist, wag
tripod SAM	1461	1468	1474	1453−1518	CH_2 scissors def
	2860	2861	2852	3022−3056	CH_2 sym. str.
	2929	2934	2925	3070−3107	CH_2 asym. str.
	∼800/∼840	800/847	794/844		**CH_3**-O− sym./asym. rocking
$Si-OCH_3$	1106	1110	1108		Si−O−C asym. str.
terminated	∼1200−1400	∼1200−1400	∼1220−1400		CH_2 wag, twist
tripod SAM	1455	1464	1468		CH_2 scissors def
	2860	2853	2851		CH_2 sym. str.
	2929	2935	2923		CH_2 asym. str.
	2980	∼2980	∼2980		**CH_3**-O− asym. str

[a] DFT was used to compute the frequencies of ME and tripod SAMs derived from it, but models of the MH or MHD monolayers were not constructed. [b] The frequencies reported are for the tripod structure shown in Figure 4c and d (vide infra). [c] Reference 35. [d] Si−Cl stretching mode for the neutral (anion) ME-tripod SAM.

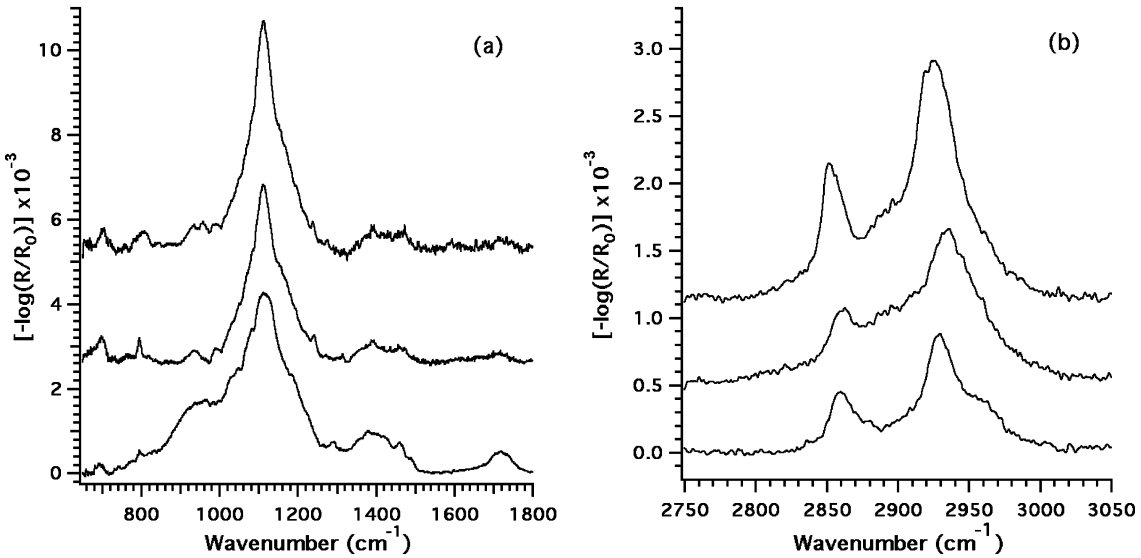

Figure 2. IRS spectra of the ME (bottom), MH (middle), and MHD (top) SAMs after reaction with $SiCl_4$ in the low (a) and high (b) frequency regions. The spectra are shifted vertically for clarity.

appearance of the methyl vibrations provides indirect evidence for the existence of the Si−Cl bond and the ability to utilize this reactive center to functionalize the tripod SAM. While a water rinse of the Si−Cl-terminated tripod SAM must yield the desired silanol functional group, the SiO−H stretching mode expected at ∼3745 cm^{-1} was not observed. The IRS spectra of the silanol-terminated tripod SAMs are quite similar to those of the methyl-terminated SAM except for the CH_3 bands.

The major change in film thickness for each monolayer occurred after reaction with $SiCl_4$ where the thickness increased by ∼2−3 Å for all SAMs, Table 2. The subsequent reaction with methanol yielded minor changes that were slightly variable between runs. The latter observation may have to do with the low density of siloxane functional groups at the monolayer surface. If all hydroxyl groups of the parent monolayers reacted with silicon tetrachloride, the density of siloxane groups would be 1/3 of the initial packing density. In practice, defects exist and it is pertinent to raise the question of what the film thickness means when small molecular fragments such as CH_3 are added to cover ∼1/3 of the surface. There has been some interest in low-density SAMs at the air−monolayer interface for particular applications, tribology for example,[42] where the tripod SAM functionalized with a long alkyl chain may prove to be advantageous because the trithiolate ligand has potential to exhibit greater mechanical stability than a monodentate one.

DFT calculations were employed to construct a physical model of the molecular tripod formed by the reaction of the 2-mercaptoethanol SAM and $SiCl_4$ and to compare the predicted SAM height with the experimentally obtained film thickness values. Recall that the unrestricted and restricted B3LYP functionals were used to describe the open-shell and closed-shell (anion) states of the tripod (vide supra). The resulting neutral and

(41) Wang, Z. Characterization and surface chemistry on model SiO_2 thin films. Ph.D. dissertation, The Pennsylvania State University, 1994.

(42) Park, J.-S.; Vo, A. N.; Barriet, D.; Shon, Y.-S.; Lee, R. T. *Langmuir*, **2005**, *21*, 2902−2911.

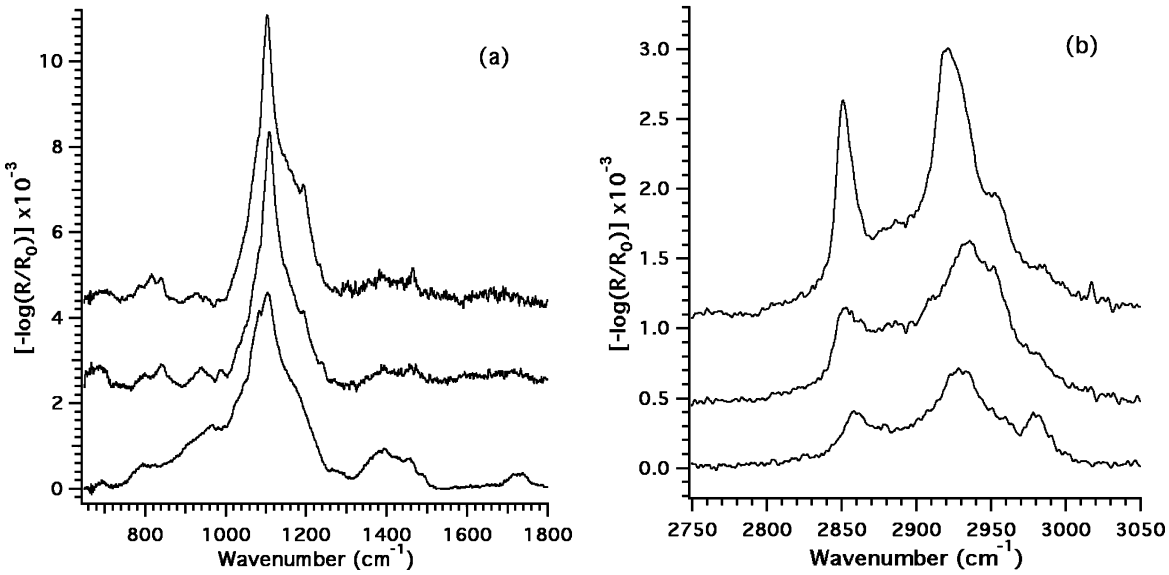

Figure 3. IRS spectra of the ME (bottom), MH (middle), and MHD (top) SAMs after reaction with $SiCl_4$ and methanol in the low (a) and high (b) frequency regions. The spectra are shifted vertically for clarity.

Table 2. SAM Thickness (Å) Determined by Single Wavelength Ellipsometry[a]

	terminal functional group		
SAM	OH	tripod(Si−Cl)	tripod(Si−OMe)
2-mercaptoethanol	5.6	8.7	8.0
6-mercaptohexanol	9.0	11.4	13.1
16-mercaptohexadecanol	23.0	25.3	25.0

[a] The average error in all values is ∼ThinSpace±1 Å.

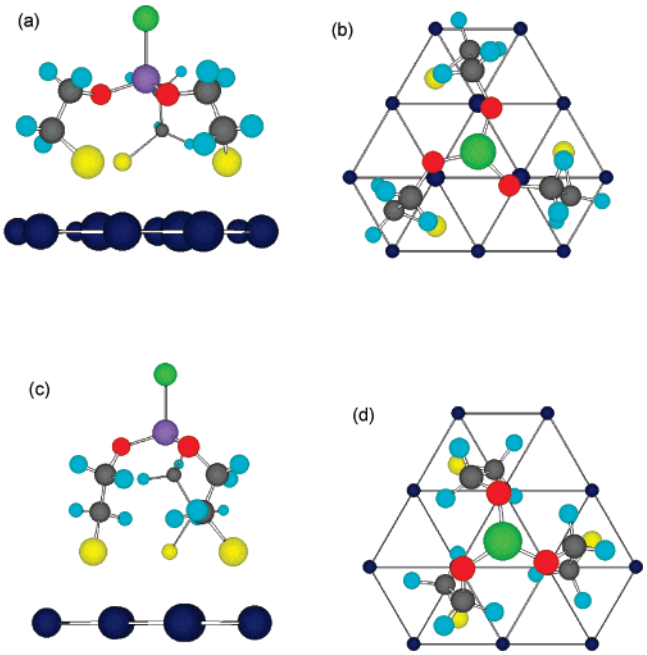

Figure 4. Perspective view of the optimized structure of the neutral (a) and negatively charged (c) molecular tripod on an idealized Au_{12} surface. Top down view of the neutral (b) and anion (d) structures. Atom types: Cl, green; Si, purple; O, red; C, gray; S, yellow; H, light blue; Au, dark blue.

negatively charged structures are shown in Figure 4. The predicted film thickness is taken as the distance from the center of the chlorine atom to the center of the planar array of gold atoms. DFT predicts a structure that extends 7.3 and 8.7 Å above the gold surface, for the neutral and anion, respectively. The latter

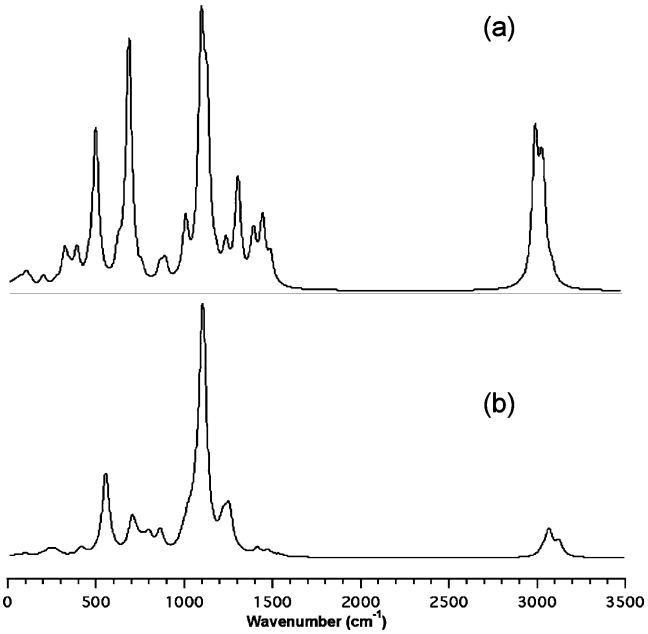

Figure 5. Computed IR spectra of the neutral (a) and anion (b) ME tripod SAM.

value for the closed shell anionic structure is in good agreement with the ellipsometry results. An inspection of the neutral structure, Figure 4a and b, reveals that the $-S-CH_2CH_2-O-$ backbone resides in a gauche configuration with a dihedral angle of 67.5°. The anion structure, Figure 4c and d, retains anti character with a dihedral angle of 163.2°. Other geometric parameters, such as, the Si−Cl, C−O, C−C, and S−C bond lengths are very similar for both structures, Table 3, and with gas-phase 2-mercaptoethanol where the appropriate comparison can be made. The largest change in bond length is the 0.15 Å increase in the gold-to-thiolate distance for the anion structure. Cartesian coordinates for all structures are included with the Supporting Information.

The calculation of the harmonic vibrational frequencies shows that neither structure is a true energy minimum. The neutral structure had four negative force constants and the anion had seven. The normal coordinates indicate that these force constants ($|\partial^2 V/\partial \mathbf{r}^2| < 0.050$ mDyne/Å) are associated with gold−sulfur and, gold−gold low-frequency vibrations along trajectories that

Table 3. Selected Bonding Parameters for the Neutral and Anion Structures of the ME Tripod SAM Computed with the UB3LYP/6-311+g and B3LYP/6-311+g** Models, Respectively**

parameter	neutral (Figure 4a, b)	anion (Figure 4c, d)	2-mercaptoethanol
Si−Cl (Å)	2.088	2.071	
Si−O (Å)	1.628	1.638	
O−C (Å)	1.426	1.443	1.428
C−C (Å)	1.529	1.528	1.521
S−C (Å)	1.845	1.836	1.846
Au plane to S (Å)	2.377	2.528	
Cl−Si−O angle	108.7°	107.3°	
O−Si−O angle	110.2°	111.6°	
O−C−C angle	110.7°	111.5°	106.7°
C−C−S angle	109.5°	111.6°	109.0°
$-S-CH_2-CH_2-O$ dihedral	67.5°	163.2°	180.0°

were frozen during the geometry optimization. A comparison of the predicted isotropic IR spectra for both structures, Figure 5, shows that the spectrum of the anion tripod, Figure 4c and d, is a much better match to the experimental IRS spectrum. The neutral structure has CH_2 stretching and deformation peaks that are too intense and not in proportion to the observed spectrum. The close match between the computed spectrum in Figure 5b and predicted film thickness to experiment suggests that the structure shown in Figure 4c is a reasonable representation of the 2-mercaptoethanol tripod SAM. Table 1 lists the harmonic frequencies computed for the anion shown in Figure 4c. The computed frequencies agree with the experimental ones, which adds further support to the proposed structure of the molecular tripod on a gold (111) surface. The largest relative errors in the calculated frequencies of the anion compared to experiment (4.8−6.8%) occur for the CH_2 stretching vibrations and are due to the absence of diffuse functions on hydrogen atoms in the 6-311+g** basis set.

The computational results raise two questions: (1) Is the neutral or anion structure a better representation for the tail group of the 6-mercaptohexanol and 16-mercaptohexadecanol tripod SAMs and (2) why should adding a single electron to a large molecule result in such a different structure? Clearly, the model used to compute structures and frequencies, a single molecular tripod on a surface represented by 12 gold atoms, does not represent the complex interactions within a monolayer. Since dispersion forces between molecules in a monolayer drive long-chain alkylthiols, such as MHD, toward organized states of self-assembly, it is reasonable to hypothesize that the reaction of $SiCl_4$ with the hydroxyl terminal groups would induce the surface states away from idealized packing configurations, but that the disorder would be restricted to methylene groups closer to the siloxane functional group and not propagate completely through the chain. Thus, Figure 4c is considered to be a better approximation of the terminal portion of the tripod structure for MH and MHD tripod SAMs while the densely packed quasi-crystalline structure persists below. It is possible that if neighboring ME tripod structures could be included in the computation of the neutral structure, dispersion forces would lead to a more upright geometry, such as that shown in Figure 4c. Since our computational resources do not permit such large-scale calculations, we are assessing the impact of electronic structure on the ME tripod geometry through additional studies that include more gold atoms to better represent the substrate, which should also mitigate the influence of added electrons.

Throughout the investigation, the Si−Cl-terminated SAM was exposed to air during sample transfer between instruments. Interestingly, the highly reactive Si−Cl bond remains intact for short periods at ambient. The stability may be a kinetic effect due to the steric constraint imposed by a densely packed surface. This observation suggests additional applications for the reactive Si−Cl-tipped tripod SAM in which the surface properties can be readily modified by reaction with a suitable nucleophile.

2-Mercaptoethanol SAMs deserve further comment in light of previous scanning tunneling microscopy (STM), surfaced enhanced Raman spectroscopy (SERS), and ATR-FTIR studies. In the STM study, the ME SAM was prepared by exposing the (111) surface of a single crystal of gold to a 10 mM ethanolic solution for 2 h, which was followed by a 1 h 80 °C annealing period.[43] The STM images show distinctive striped patterns that were identified as combinations of molecular assemblies based on nonequivalent $(\sqrt{3} \times \sqrt{3})R30°$ structural units.[43] One of the few IR studies prepared ME SAMS from 0.64 M ethanol solutions with a maturation period of 24 h.[44] The film thickness was not reported and the peak positions differ somewhat from those reported in Figure 1 and Table 1. Our experience suggests that ME solutions with relatively high concentrations >10 mM can result in multilayered ME structures on gold as determined by ellipsometry. However, the multilayer may be reduced to approximately a monolayer by heating at 80 °C in an oven for 1−2 h. A recent study employed SERS to examine the trans/gauche ratio of ME SAMs on Au, Ag, and Cu.[45] For this work, electrochemically roughened substrates were soaked in 10 mM ME/ethanol solutions for 2−24 h. A significant population of gauche conformations was found with an average ratio of 1:1.9 gauche to trans conformations for ME SAMs on gold.

In our initial study of ME monolayers, we observed that short incubation times of about 1 day usually lead to IRS spectra in which the CH_2 stretching bands had greater intensity than the C−O stretch, which contrasts with the densely packed SAM characterized by the spectrum in Figure 1. The film thickness was also highly variable but typically shorter, 3.5−5.0 Å, than densely packed ME monolayers. The origin of these intensity shifts may involve a significant contribution from gauche conformations. A relatively large population of gauche conformations is consistent with the observations of the SERS[45] and especially STM[43] work, although the latter study did not include vibrational spectra or film thickness measurements. In summary, densely packed 2-mercaptoethanol SAMS adopt a largely all-trans conformation after 4 days in dilute 2 mM ethanol solutions and lead to reproducible IRS spectra and film thickness measurements.

One of the unusual aspects of 2-mercaptoethanol compared to MH or MHD was the observation of a distinct carbonyl stretching band at 1720 cm^{-1} in all IRS spectra that were prepared in air saturated solutions, Figure 1a. In a separate experiment, the ME SAM was formed from the pure vapor under a nitrogen

(43) Hyun, M.; Rhee, C. K. *Bull. Kor. Chem. Soc*. **2001**, *22* (2), 213−218.
(44) Zhang, X. H.; Wang, S. F. *Sensors* **2003**, *3*, 61−68.
(45) Kudelski, A. *J. Raman Spectrosc*. **2003**, *34*, 853−862.

atmosphere. Although this particular film consisted of a thick ~50 Å multilayer, no carbonyl stretching bands were observed. When this sample was heated in an oven at 80 °C for an hour in air, a film close to the expected monolayer thickness, ~8 Å, remained and the carbonyl band was observed. The short chain of ME places the hydroxyl group in close proximity to the gold surface especially in the gauche conformation. Recent reports have shown that gold nanoparticles can function as oxidative catalysts at ambient temperature and that low coordination gold atoms at edges and corners are likely reactive sites.[46] Since the substrate is a polycrystalline gold surface with ~2 nm rms roughness and the ME SAM is kinetically slow to form by comparison to MH and MHD SAMs, which are essentially in their final form after ~1 day, it is possible that oxidation of the hydroxyl group occurs on gold in the presence of adsorbed oxygen or water.[47]

Conclusions

Taken together, the IRS, SWE, and DFT results strongly support the proposed structure of a molecular tripod SAM. This procedure is unique in that the tripod structure is easily formed from a densely packed SAM in one step and avoids time-consuming synthesis and purification of molecules that contain multiple thiol groups. In addition, the trithiolate structure may impart thermal and mechanical stability above that normally found for monolayers composed of molecules with single RS−Au surface bonding interactions. The thermal stability is currently under investigation. In terms of our original goal of developing an organic interface to facilitate studies of zeolite films, the tripod SAM appears to be an excellent candidate. In forthcoming work, it will be demonstrated that the tripod SAM is suitable substrate for the chemical attachment and growth of zeolite films. By changing the length of the alkyl chain or by substituting aryl for alkyl spacers, the properties of the monolayer may be tailored to obtain a particular electrical response, which is highly relevant to conductivity measurements of alkali metal-doped zeolite films, M@SZ.

The scope of the chemistry described in Scheme 1 is not limited to the reaction of $SiCl_4$ with mercapto-alcohols. The use of amine-terminated thiols, $HS-R-NH_2$, offers intriguing possibilities for SAM development. In addition, other reactive compounds such as $TiCl_4$ may form Ti-terminated tripod SAMs, respectively, that could be used to grow titania films covalently attached to a surface. Work on Ti−Cl-terminated tripod SAMs and their use to prepare titania films is in progress.

Acknowledgment. This work was supported in part by the American Chemical Society Petroleum Research Fund No. 38397-GB5 and Research Corporation Cottrell Science Award No. CC5646 (ASI). A.S.I. acknowledges receipt of the SFSU Presidential award for pretenure sabbatical taken at PSU. W.L. acknowledges receipt of a GAANN fellowship; U.S. Department of Education P200A010206.

Supporting Information Available: Cartesian coordinates for the Si−Cl tipped tripod SAM (neutral and anion structures) and 2-mercaptoethanol. This material is available free of charge via the Internet at http://pubs.acs.org.

LA703196B

(46) Janssens, T. V. W.; Clausen, B. S.; Hvolbaek, B.; Falsig, H.; Christensen, C. H.; Bligaard, T.; Norskov, J. K. *Top. Catal.* **2007**, *44*, 15−26.

(47) Gong, J.; Ojifinni, R. A.; Kim, T. S.; Stiehl, J. D.; McClure, S. M.; White, J. M.; Mullins, C. B. *Top. Catal.* **2007**, *44*, 57−63.